Available online at www.sciencedirect.com
SCIENCE DIRECT®
ELSEVIER
Polymer 46 (2005) 3318–3322
polymer
www.elsevier.com/locate/polymer

Dependence of the phase separation process on the relative onset of network formation in simultaneous interpenetrating polymer networks

Jean-Michel Widmaier*, Alexandra Nilly, Jean-Marc Chenal, André Mathis

Institut Charles Sadron, UPR 0022, CNRS, 6 rue Boussingault, 67083 Strasbourg, France

Received 4 June 2004; received in revised form 13 December 2004; accepted 14 February 2005
Available online 21 March 2005

Abstract

Morphology development during the synthesis at room temperature of an interpenetrating polyurethane/poly(methyl methacrylate) network was investigated by small-angle X-ray scattering in relation with their relative kinetics of formation, determined by Fourier transform infra red spectroscopy. When the time lag between the onset of the two reactions is short, macroscopic phase separation occurs as the polyurethane network is incompletely formed. However, when the time lag increases, the poly(methyl methacrylate) forms into a more continuous network which limits the growth of phase separation to a close environment.

Keywords: Interpenetrating polymer network (IPN); Small angle X-ray scattering (SAXS); Polyurethane

---

1. Introduction

Interpenetrating polymer networks (IPNs) are combination of two crosslinked polymers, chemically distinct, held together by permanent entanglements. According to Sperling [1], IPNs are referred by their methods of synthesis, and are classified in two main groups: (i) sequential IPNs, which are prepared by a two-step process consisting in swelling first a preformed network by a second monomer subsequently polymerized and crosslinked; (ii) simultaneous IPNs, which are obtained from the initial homogeneous mixture of both network precursors, reacting selectively via non-interfering routes, typically a step-growth mechanism and a chain polymerization. For example, polyurethane/poly(methyl methacrylate) (PU/PMMA) simultaneous IPNs have been extensively studied [2–8]. However, the term simultaneous IPN is not appropriate to describe the formation process governing the phase-separated structure, responsible of the ultimate properties, since both reaction profiles are basically different, excluding true simultaneity in the building of the tridimensional structure. Therefore, we have introduced the term in situ IPNs [9] which better reflects the one-shot process instead of simultaneous IPNs. Thus, IPNs differing from a kinetic point of view are called in situ simultaneous IPNs and in situ sequential IPNs, respectively. In the first case, after mixing, both reactions are initiated at the same time whereas in the second case, polymerization and crosslinking of the second monomer occur after completion of the first network. Everythings being identical, these materials exhibit quite different morphologies, based on the well-known transparency criterion: in situ simultaneous PU/PMMA IPNs are opaque, indicating macro-phase separation whereas in situ sequential PU/PMMA IPNs are highly transparent materials, indicating at least micro-phase separation with domain size smaller than the visible wavelengths.

The aim of this paper is to provide some description of how morphology develops from the initial mixture to the final IPN, especially to get an insight into the region where the extent of phase separation changes of scale, going from macro- to micro-phase separation. This was achieved by initiation of the polymerization of methyl methacrylate at various degrees of conversion of polyurethane, especially in the PU pre-gel region, as we have already shown that starting the formation of the second network either immediately after gelation of PU, ca. 70% conversion, or well after (>98%) leads to a rather identical

---

* Corresponding author. Tel.: +33 3 88 41 40 76; fax: +33 3 88 41 40 99.

E-mail address: jmw@ics.u-strasbg.fr (J.-M. Widmaier).

0032-3861/$ - see front matter © 2005 Elsevier Ltd. All rights reserved.
doi:10.1016/j.polymer.2005.02.082

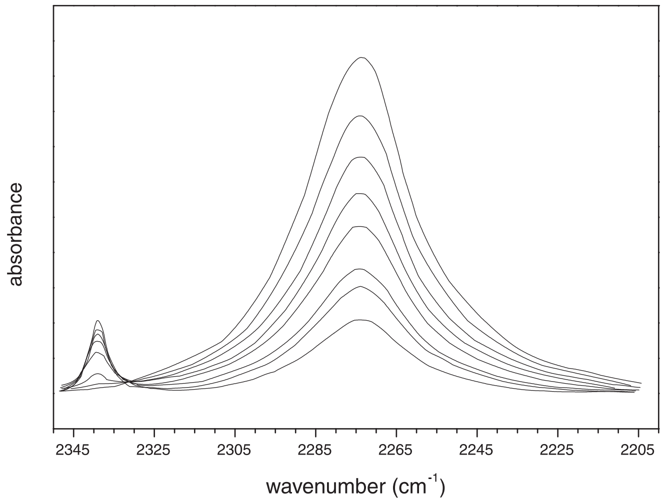

Fig. 1. Gradual disappearance of the NCO stretching absorption band at 2275 cm^{-1} in the course of PU formation.

phase-separated material [10]. We introduce the term in situ delayed IPN to describe these particular IPNs obtained with an interval of time between the onset of the two independent reactions. Formation of in situ delayed PU/PMMA IPNs was performed at room temperature, using appropriate organotin catalyst and photoinitiator. Kinetics of network formation and development of morphology were investigated by Fourier transform infra-red spectroscopy and small-angle X-ray scattering.

2. Experimental

2.1. Materials

All materials used in this study were dried appropriately, but not otherwise purified. The aromatic pluriisocyanate (Desmodur L75, Bayer) is a toluene diisocyanate/trimethylolpropane adduct dissolved in 25 wt% ethyl acetate to reduce viscosity. The NCO content was determined by standard titration using di-*n*-butylamine. The macrodiol, poly(oxypropylene glycol) (Arcol 1020, ARCO Chemicals), $M_w = 1950$ g/mol, functionality, f_n, equal to 2, was dried and degassed at 60 °C under vacuum overnight before use. Dibutyltin dilaurate (Kosmos 19, Goldschmidt) was stored in a refrigerator before use as a catalyst. The monomers, methyl methacrylate (MMA, Merck) and 1,1,1-trimethylolpropane trimethacrylate (TRIM, Degussa) were stored over 4 Å molecular sieves for at least two weeks prior to use. Their inhibitor, methylethyl hydroquinone, approximately 100 ppm, was not removed. Benzoin isobutyl ether (BzIE, Aldrich), was used as radical photoinitiator for the copolymerization of methacrylates.

2.2. Synthesis

In situ PU/PMMA IPNs were obtained at room temperature by the following procedure: to a homogeneous mixture of appropriate amounts of pluriisocyanate, macrodiol, monomers and initiator, 0.35 wt% of the organotin catalyst was added last. After rapid stirring, the mixture is injected in a sealed mold made of either two NaCl plates or mica discs for FTIR and SAXS experiments, respectively. The PU network, which forms first in the dark, is obtained by end-linking of the hydroxy groups of the macrodiol with the pluriisocyanate, using a molar ratio [NCO]/[OH] equal to 1.07, according to Tabka et al. [11]. The formation of in situ delayed IPNs was started at given times after the onset of the polyaddition reaction, simply by switching on the UV light (365 nm). The concentration of the photoinitiator was 3 wt% and the amount of TRIM was 5 wt% (based on the weight of MMA). In this study, the PU/PMMA composition was 34/66 by weight.

2.3. Methods

Fourier transform infra-red (FTIR) spectra were recorded on a Nicolet 60SX spectro-photometer equipped with a modified chamber which allows the sample being exposed to UV light. An external UV light source (UVP SpotCure, 400 W L2 lamp) equipped with a flexible guide filled with a light-conducting liquid, positioned at an angle of 60° to the NaCl window, was used to irradiate the sample. The intensity on the surface was 7 mW/cm^2 in this geometry. Scanning resolution was 2 cm^{-1} and 32 consecutive scans were averaged in the absorption mode. Small-angle X-ray scattering (SAXS) experiments were performed at room temperature, on a home-made apparatus using Cu K_α radiation (wavelength = 0.154 nm). The previous UV light source and guide were used to irradiate the sample while being exposed to X-rays. The signal was detected by a position-sensitive one-dimensional counter in a scattering vector range of 0.2–3.5 nm^{-1}. X-ray patterns were recorded every 10–12 min with an exposure time of 10 min.

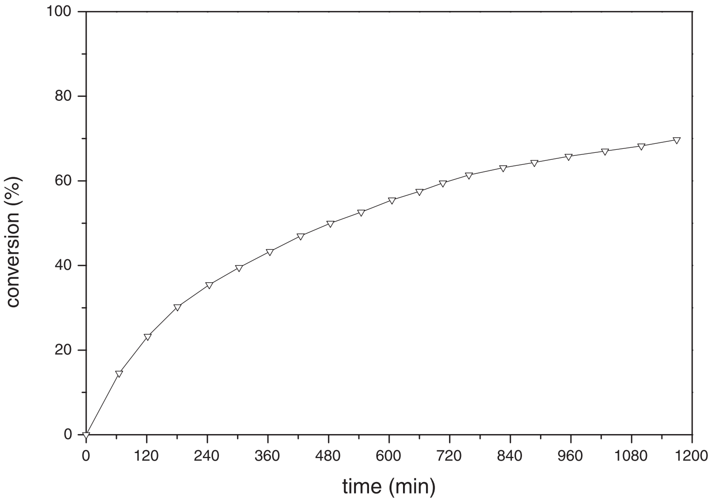

Fig. 2. Kinetics of PU formation determined by FTIR.

3. Results and discussion

3.1. Formation of the PU network

The formation of in situ PU/PMMA IPNs always begins first by the initiation of the step-growth polymerization. FTIR is an appropriate tool for kinetic measurements and structure determination of polyurethane. The progress of the reaction between the macrodiol and the pluriisocyanate was followed by monitoring the change in intensity of the absorption band for the NCO stretching vibration at 2275 cm^{-1} (Fig. 1). Integrated absorbances were corrected from sample thickness changes using the C–H peak at 2870 cm^{-1} as internal standard (reference). Thus, the time-dependent conversion, $P(t)$, can be expressed as:

$$P(t) = 1 - \frac{(A_{\mathrm{NCO}}/A_{\mathrm{ref}})_t}{(A_{\mathrm{NCO}}/A_{\mathrm{ref}})_0}$$

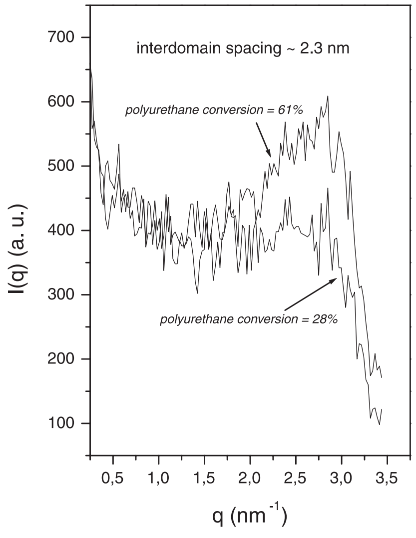

Fig. 3. Evolution of SAXS profile with PU conversion.

with A_{NCO} as the absorbance of the NCO peak and A_{ref} as the reference peak (C–H vibration), the subscript 0 corresponds to initial time. The amount of catalyst (dibutyltin dilaurate) was taken such, as the formation rate of polyurethane is relatively low at room temperature. The consumption of the isocyanate group as a function of time is shown in Fig. 2. Typically, gelation of the medium was obtained after approximately 24 h.

Other relevant peaks in polyurethanes are in the 3200–3500 and 1680–1750 cm^{-1} regions, corresponding to –NH and –C=O vibrations, respectively. The changes (intensity, shift) of the peaks in these two regions are indicative of interatomic interactions between adjacent urethane groups, and can provide information to estimate the extent of micro-phase separation. The absorption peak located at 3325 cm^{-1} corresponds to hydrogen-bonded –NH groups whereas the peak at 3375 cm^{-1} is attributed to free non-bonded –NH groups. Similarly, the peak at 1705 cm^{-1} is assigned to the hydrogen-bonded –C=O stretching band, while that at 1735 cm^{-1} is assigned to free –C=O groups. The ratio of bonded groups over non-bonded groups suggests the extent of micro-phase separation. At early reaction times, two well-defined peaks are seen in the –NH region. In the course of the reaction, the absorption of the free –NH groups is reduced into a small shoulder whereas the peak corresponding to the bonded –NH groups becomes stronger and larger, indicating greater micro-phase separation. Unfortunately, a quantitative estimation cannot be given due to the presence of ethyl acetate and pre-existing urethane groups in the pluriisocyanate adduct. This also concerns the carbonyl region. Note that during the PU formation, the intensity of the strong C=C stretching band at 1640 $\mathrm{cm}^{-1}$of methyl methacrylate monomer remains unchanged.

Information about the formation of the PU network is provided by SAXS studies, considering the development of the well-known micro-phase separation into 'soft' and 'hard' phases occurring during polymerization.

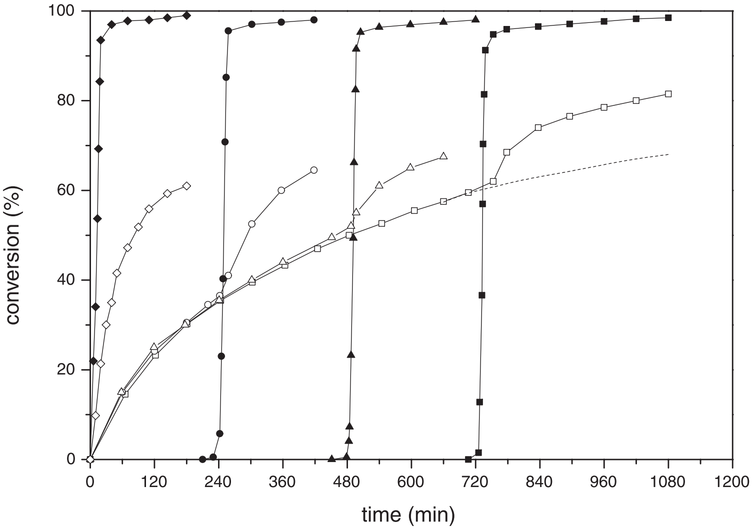

Fig. 4. Kinetics of in situ delayed PU/PMMA IPN formation (♦,◇) simultaneous onset of both reactions; (●,○), initiation of free-radical polymerization delayed 4 h; (▲,▽), time lag, 8 h; (■,□), time lag, 12 h. Full symbols refer to MMA polymerization, and open symbols to PU.

Progressively, a maximum appears on the plot of intensity, $I(q)$, versus scattering vector, q, suggesting the formation of a periodic structure within the sample (Fig. 3). The interdomain spacing, d, which only depends on the molecular weight of the macrodiol, was estimated using Bragg's law to be equal at a value of $d = 2.3$ nm. As expected from the use of an end-linking process for the formation of the PU network, the d spacing does not change in the course of network formation, only the scattering intensity, $I(q_{\max})$, increases with NCO conversion, showing a better resolution with time of the PU network structure.

3.2. Formation of in situ delayed IPNs

Three different in situ delayed IPNs were obtained by initiating the polymerization of MMA at various times in the growing polyurethane pre-gel region, as seen on Fig. 4. Despite the rapid polymerization of MMA the formation of the PU network is not stopped. The kinetic profiles clearly show an increase in the step polymerization rate, due to the exothermal free radical polymerization, which locally increases temperature of the reactive medium. The acceleration of the pluriisocyanate–macrodiol reaction may also be a consequence of the UV irradiation, and a possible subsequent increase of the catalytic activity of DBTDL resulting from an eventual change in the electronic state of the intermediary complex which would faster decompose.

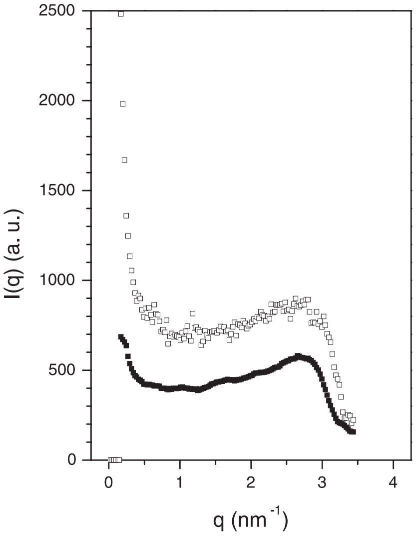

Fig. 5. SAXS pattern of PU in the pre-gel region (~45% conversion), (■) neat PU; (□) while forming PMMA. The curve data correspond to the mean value of three adjacent data sets.

Like previously for the formation of neat polyurethane, SAXS data were used to investigate the phase separation process while forming IPNs. At the onset of the in situ polymerization of MMA, a fast increase of the global scattering intensity is observed (Fig. 5), however, particularly marked in the low q region (0.2–0.5 nm^{-1}), together with a small shift of $q_{\max}$ toward lower values of q. That shift can be interpreted as an increase of the average distance between PU crosslinks. Therefore, it may be assumed that the PU network chains are stretched because of the polymerization of MMA and that a high degree of mixing would result. $q_{\max}$ shifts versus PU conversion.

The increase in scattering intensity due to the IPN formation can be related to the degree of phase separation via the relative Porod's invariant Q' [12]. Values of Q' correspond to the integration of $q^2I(q)$ versus q curves between the first and last data points:

$$Q' = \int_0^\infty q^2 I(q)\mathrm{d}q$$

This invariant can be related to the volume fraction φ_i and electronic density ρ_i of the phases i as

$$Q' \propto \varphi_1\varphi_2(\rho_1 - \rho_2)^2$$

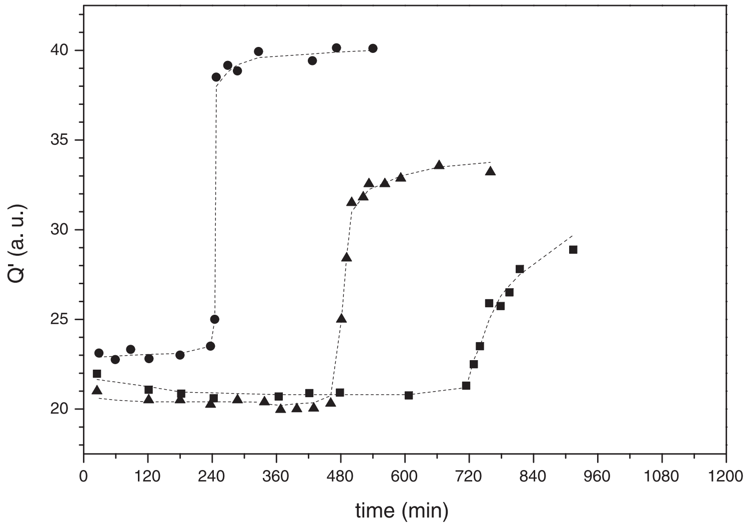

Fig. 6. Plots of the relative invariant, Q', as a function of time for various in situ delayed IPNs (●) time lag, 4 h; (▲) time lag, 8 h; (■) time lag, 12 h.

in the case of a two-phase system, where the subscripts 1 and 2 refer to phase 1 and 2, respectively. Plots of Q' versus time for the three in situ delayed IPNs are shown in Fig. 6. Each plot exhibits three distinct regions: an initial plateau followed by a marked jump and finally another plateau with an almost constant value of Q', the latter depending on the time of initiation of MMA polymerization. The rapid increase in Q' corresponds to the onset of phase separation between polyurethane and poly(methyl methacrylate) being formed, and the steepness of the jump reflects the facility to bring the medium to phase separation. The end value of Q' gives an estimation of the extent of polymerization-induced phase separation: when the polyurethane is loose with only a few topological restraints (~30% conversion), phase separation occurs very rapidly and expand mainly under thermodynamic control similarly to what would occur to polymer blends. The result of this is that the material exhibits a macro-phase separated morphology confirmed by its milky-like aspect. On the other hand, when polymerization of MMA occurs in the presence of a polyurethane close to its gel point, i.e. ca. 70% conversion, gross phase separation is impeded due to rheological and topological reasons. In that case, the sample exhibits optical clarity, slightly less than that of an in situ sequential IPN (for which the onset of MMA polymerization takes place well after completion of PU).

4. Conclusion

In this paper, we have introduced in situ delayed PU/PMMA IPNs which are a sub-class of the so-called simultaneous IPNs classically prepared from an initial reactive mixture of the components which are polymerized via different reaction mechanisms. By simply varying the lap time between the onset of the two reactions, quite different morphologies, and hence properties, were obtained for a given composition. When formation of PMMA occurred in the presence of a badly built PU network, a macro-phase separated IPN is obtained whereas only micro-phase separation is possible when entanglements are pre-existing in the reactive medium.

References

[1] Sperling LH. Interpenetrating polymer networks and related materials. New York: Plenum Press; 1981.
[2] Xiao HX, Frisch KC, Frisch HL. J Polym Sci Polym Chem Ed 1983; 21:2547.
[3] Jehl D, Widmaier JM, Meyer GC. Eur Polym J 1983;17:597.
[4] Hermant I, Damyanidu M, Meyer GC. Polymer 1983;24:1419.
[5] Jin SR, Widmaier JM, Meyer GC. Polymer 1988;29:346.
[6] Roha M, Wang B. J Appl Polym Sci 1992;45:1367.
[7] Akay M, Rollins SN. Polymer 1993;34:1865.
[8] Mishra V, DuPrez FE, Goethals E, Sperling LH. J Appl Polym Sci 1995;58:371.
[9] Tabka MT, Widmaier JM, Meyer GC. Plast Rubber Process Appl 1991;16:11.
[10] Abetz V, Meyer GC, Mathis A, Picot C, Widmaier JM. Polym Adv Technol 1996;7:295.
[11] Tabka MT, Widmaier JM, Meyer GC. Macromolecules 1989;22: 1826.
[12] Chu B, Gao T, Li Y, Wang J, Desper CR, Byrne CA. Macromolecules 1992;25:5724.